



Higher Atmospheric CO₂ Levels Favor C₃ Plants Over C₄ Plants in Utilizing Ammonium as a Nitrogen Source

Feng Wang^{1,2,3*}, Jingwen Gao^{1,3}, Jean W. H. Yong^{3,4}, Qiang Wang¹, Junwei Ma^{1*} and Xinhua He^{2,3*}

¹ Institute of Environmental Resources, Soil and Fertilizer, Zhejiang Academy of Agricultural Sciences, Hangzhou, China,

² Centre of Excellence for Soil Biology, College of Resources and Environment, Southwest University, Chongqing, China,

³ School of Biological Sciences, The University of Western Australia, Perth, WA, Australia, ⁴ Department of Biosystems and Technology, Swedish University of Agricultural Sciences, Alnarp, Sweden

OPEN ACCESS

Edited by:

Fulai Liu,
University of Copenhagen, Denmark

Reviewed by:

Zhaozhong Feng,
Research Center
for Eco-environmental Sciences
(CAS), China
Xiancan Zhu,
Anhui Normal University, China
Xiangnan Li,
Northeast Institute of Geography
and Agroecology, Chinese Academy
of Sciences, China

*Correspondence:

Feng Wang
wangfeng@zaas.ac.cn
Junwei Ma
majw@zaas.ac.cn
Xinhua He
xinhua.he@uwa.edu.au

Specialty section:

This article was submitted to
Plant Nutrition,
a section of the journal
Frontiers in Plant Science

Received: 24 February 2020

Accepted: 05 November 2020

Published: 02 December 2020

Citation:

Wang F, Gao J, Yong JWH,
Wang Q, Ma J and He X (2020)
Higher Atmospheric CO₂ Levels Favor
C₃ Plants Over C₄ Plants in Utilizing
Ammonium as a Nitrogen Source.
Front. Plant Sci. 11:537443.
doi: 10.3389/fpls.2020.537443

Photosynthesis of wheat and maize declined when grown with NH₄⁺ as a nitrogen (N) source at ambient CO₂ concentration compared to those grown with a mixture of NO₃⁻ and NH₄⁺, or NO₃⁻ as the sole N source. Interestingly, these N nutritional physiological responses changed when the atmospheric CO₂ concentration increases. We studied the photosynthetic responses of wheat and maize growing with various N forms at three levels of growth CO₂ levels. Hydroponic experiments were carried out using a C₃ plant (wheat, *Triticum aestivum* L. cv. Chuanmai 58) and a C₄ plant (maize, *Zea mays* L. cv. Zhongdan 808) given three types of N nutrition: sole NO₃⁻ (NN), sole NH₄⁺ (AN) and a mixture of both NO₃⁻ and NH₄⁺ (Mix-N). The test plants were grown using custom-built chambers where a continuous and desired atmospheric CO₂ (C_a) concentration could be maintained: 280 μmol mol⁻¹ (representing the pre-Industrial Revolution CO₂ concentration of the 18th century), 400 μmol mol⁻¹ (present level) and 550 μmol mol⁻¹ (representing the anticipated futuristic concentration in 2050). Under AN, the decrease in net photosynthetic rate (*P_n*) was attributed to a reduction in the maximum RuBP-regeneration rate, which then caused reductions in the maximum Rubisco-carboxylation rates for both species. Decreases in electron transport rate, reduction of electron flux to the photosynthetic carbon [*Je(PCR)*] and electron flux for photorespiratory carbon oxidation [*Je(PCO)*] were also observed under AN for both species. However, the intercellular (*C_i*) and chloroplast (*C_c*) CO₂ concentration increased with increasing atmospheric CO₂ in C₃ wheat but not in C₄ maize, leading to a higher *Je(PCR)/Je(PCO)* ratio. Interestingly, the reduction of *P_n* under AN was relieved in wheat through higher CO₂ levels, but that was not the case in maize. In conclusion, elevating atmospheric CO₂ concentration increased *C_i* and *C_c* in wheat, but not in maize, with enhanced electron fluxes towards photosynthesis, rather than photorespiration, thereby relieving the inhibition of photosynthesis under AN. Our results contributed to a better understanding of NH₄⁺ involvement in N nutrition of crops growing under different levels of CO₂.

Keywords: atmospheric CO₂, ecophysiology, electron transport, NH₄⁺ stress, photosynthesis, *Triticum aestivum*, *Zea mays*

INTRODUCTION

The application of chemical nitrogen (N) fertilizers has greatly increased global crop yields and decreased world hunger over the past five decades (Gong et al., 2011). However, only 30–40 % of applied N is utilized by crops; most is lost in numerous ways, including run-off, leaching, denitrification and volatilization, which together lead to a range of environmental problems (Richter and Roelcke, 2000; Xing and Zhu, 2000). Thus, increasing plant nitrogen use efficiency (NUE) is crucial for the development of sustainable agriculture. Unlike nitrate (NO₃⁻), ammonium (NH₄⁺) can be assimilated by plants without further chemical reduction (Mehrer and Mohr, 1989; Onoda et al., 2004). NH₄⁺ can be provided by both manure and urea fertilizers (Xu et al., 2012; Coskun et al., 2017). A promising future strategy for improving agronomic NUE is the application of stabilized-NH₄⁺-based fertilizers together with other active compounds, such as nitrification inhibitors, which can inhibit the nitrification of NH₄⁺, thereby maintaining a high soil N content in the form of NH₄⁺ over extended periods (IPCC, 2007; Ariz et al., 2011). Some crops, including wheat and maize, are able to grow well when provided with a mixture of NO₃⁻ and NH₄⁺ (Mix-N), or NO₃⁻ as the sole N source (NN) (Miller and Cramer, 2005). Under certain environmental conditions, NH₄⁺ may reduce growth by decreasing photosynthesis, thereby lowering crop productivity (Britto and Kronzucker, 2002). Since urea and NH₄⁺-based N fertilizers are used commonly to support the growth of cereals, vegetables and fruits, a better understanding of the toxic effects of NH₄⁺ in plant nutrition should facilitate better crop productivity (Miller and Cramer, 2005; Fernández-Crespo et al., 2012).

Photosynthesis is a synergistic process that involves electron harvesting, transport, and utilization (Kühlbrandt et al., 1994). Photosynthetic electron transport typically involves two reaction centers: photosystems I and II (PSI and PSII, respectively). The D1 protein of PSII is sensitive to NH₄⁺, and a loss of PSII function occurs when NH₄⁺-based fertilizers are applied

in excessive quantities (Drath et al., 2008). When this occurs, impairment of the photosynthetic electron transport chain will lead to a decrease in photochemical efficiency (Φ_{PSII}) and the electron transport rate (J_e), in turn leading to a deficiency in NADPH and ATP for CO₂ assimilation (Wang et al., 2019). The atmospheric CO₂ concentration (C_a) has increased from 280 $\mu\text{mol mol}^{-1}$ in pre-industrial times to 400 $\mu\text{mol mol}^{-1}$ at present, and is expected to reach 550 $\mu\text{mol mol}^{-1}$ by the 2050 s (IPCC, 2013). The elevation of CO₂ concentration at the sites of Rubisco carboxylation alters plant photosynthetic sensitivity, potentially modulating sensitivity to a diversity of N sources. Due to the importance of food production security and crops in the global carbon cycle, an improved understanding of C_a changes on the N nutrition of C₃ and C₄ plants will become more and more crucial (Lloyd and Farquhar, 1996; Ghannoum et al., 2000). In general, plants with the C₄ photosynthetic pathway have anatomical and biochemical traits that increase CO₂ levels around the carboxylating Rubisco enzyme (Hatch and Slack, 1966). Bloom et al. (2014) and Dier et al. (2018) showed that NO₃⁻ assimilation is inhibited by elevated CO₂ concentrations in field-grown C₃ wheat plants. We postulated that an elevated C_a increases photosynthesis to produce more carbon skeletons, which in turn would increase NH₄⁺ assimilation, thereby ameliorating the possible physiological stress of having excess free NH₄⁺ in C₃ plants. The detailed comparative physiological responses of C₃ and C₄ plants to NH₄⁺ fertilization under elevated C_a are still not fully understood (Bloom et al., 2002, 2010; Cousins and Bloom, 2003; Bloom, 2015).

A wide variety of equipment, including open-top chambers (OTC), controlled-environment (CE) systems, and free-air CO₂ enrichment (FACE) systems, has been used to study the effects of elevated C_a . In the OTC system, plants are held in a chamber with an open top that facilitates gas exchange with the atmosphere (Owensby et al., 1999). However, the temperature is generally higher inside the chamber than outside, inevitably increasing plant transpiration, which influences plant growth rates. The FACE system minimally perturbs the plant growth environment and is suitable for long-term experiments under elevated C_a . However, the FACE system could not be used to study the effects of sub-ambient CO₂ concentrations. Controlled environment experiments can also be performed in greenhouses and artificial growth chambers (Yong et al., 2000; Aranjuelo et al., 2009; Kanemoto et al., 2009; Robredo et al., 2011). To design a system having minimal impact on natural temperature, light and seasonality, while also having the capacity to provide either sub-ambient or elevated levels of CO₂, we custom-fabricated experimental chambers in which the inside temperature and humidity were kept similar to outside open field conditions while regulating the C_a .

Our primary objective was to improve understanding of (i) the physiological mechanisms underlying the photosynthetic inhibition caused by NH₄⁺ nutrition and (ii) the mechanism by which C_a affects the NH₄⁺ tolerance of C₃ and C₄ plants. We therefore studied the photosynthetic responses of a C₃ plant (wheat, *Triticum aestivum* L.) and a C₄ plant (maize, *Zea mays* L.). Both these species prefer NO₃⁻ as the N nutrient source and we grew them under three C_a concentrations (280, 400, or 550 $\mu\text{mol mol}^{-1}$) combined with three forms of N

Abbreviations: Γ^* , the CO₂ compensation point related to C_i; ϕ , apparent quantum yield; Φ_{PSII} , quantum efficiency of PSII; C_a , atmospheric CO₂ concentration; C_c , chloroplastic CO₂ concentration; CE, carboxylation efficiency; C_i, intercellular CO₂ concentration; C_m, CO₂ concentrations in the mesophyll cells; C_s, CO₂ concentrations in the bundle sheath; C treatment, the CO₂ concentration treatment of each sample; FACE, free-air CO₂ enrichment; F_m, the maximum chlorophyll fluorescence with dark-adaptation; F_m' the maximum fluorescence with light-adaptation; F_o, the minimum chlorophyll fluorescence with dark-adaptation; F_o' the minimum chlorophyll fluorescence with light-adaptation; F_s, steady state fluorescence with light-adaptation; F_v/F_m, maximum quantum efficiency of PSII; g_m, mesophyll conductance; g_s, stomatal conductance; J_a, alternative electron flux; J_{cmax}, maximum carboxylation rates limited by RuBP regeneration; J_e(PCO), electron fluxes to photosynthetic carbon oxidation; J_e(PCR), electron fluxes to photorespiratory carbon reduction; J_{max}, maximum electron transport rates; LHC, light-harvesting complex; Mix-N, a mixture of both NO₃⁻ and NH₄⁺ source; NPQ, non-photochemical quenching; NUE, nitrogen use efficiency; OTC, open-top chambers; P_n, net photosynthetic rate; PPFED, photon flux intensity; PSII, photosystem II; PVC, polyvinyl chloride; qL, photochemical quenching; R_d, mitochondrial respiration rate in the light; ROS, reactive oxygen species; Rubisco, ribulose-1,5-bisphosphate carboxylase/oxygenase; v_c, the carboxylation rate; V_{cmax}, maximum carboxylation rate limited by Rubisco; v_o, the oxygenation rate; V_{pdl}, the vapor pressure deficit; V_{pmax}, the maximal rate of PEP carboxylation; w_c, the potential Rubisco carboxylation rate; w_j, the potential RuBP regeneration rate; w_p, the potential triose-phosphate utilization rate.

nutrition: Mix-N, NN and sole NH₄⁺ nitrogen (AN). Our other objective was to provide new knowledge facilitating (i) directed breeding programs aiming to produce N-efficient cultivars, and (ii) the development of sustainable crop N management strategy to adapt to a future with elevated C_a, as predicted by current models of global climate change.

MATERIALS AND METHODS

Plant Materials and Experimental Design

Wheat (*T. aestivum* cv. Chuanmai 58) and maize (*Z. mays* cv. Zhongdan 808), two common crop species in Chongqing, China, were grown under hydroponic experimental conditions. Seeds of both species, of uniform size, were sterilized in 20% (v/v) H₂O₂ for 10 min, rinsed with distilled water, and germinated in darkness in culture dishes covered with wet sterile gauze. When the cotyledons were 1.0 cm long, the seedlings were transferred to silica sand (previously soaked in 1% HCl for 2 days, followed by flushing with copious amounts of water to remove all traces of HCl) and watered twice daily with distilled water. Uniform 14-day-old (two-leaf stage) seedlings were transplanted into opaque plastic growth containers containing a modified Hoagland's solution (Wang et al., 2016a; Gao et al., 2018), with three N sources: Mix-N, NN or AN. The composition of the Mix-N solution was as follows: macronutrients were provided as 5.0 mM N in the form of Ca(NO₃)₂, KNO₃ and (NH₄)₂SO₄ (the ratio of NO₃⁻ to NH₄⁺ in the Mix-N was 3 : 2), 3.0 mM K in the form of KH₂PO₄ and KNO₃, 1.5 mM Ca as Ca(NO₃)₂ and CaCl₂, 1.0 mM Mg as MgSO₄, 1.0 mM P as KH₂PO₄, and 0.6 mM Na as NaCl. Micronutrients were provided as 0.1 mM Fe as Fe-EDTA, 455 × 10⁻³ mM Mn as MnSO₄, 38.1 × 10⁻⁶ mM Zn as ZnSO₄, 15.6 × 10⁻⁶ mM Cu as CuSO₄, 2.31 × 10⁻³ mM B as H₃BO₃, and 6.2 × 10⁻⁶ mM Mo as MoO₃. Macronutrients were provided in the NO₃⁻-source solution as 5.0 mM N in the form of Ca(NO₃)₂ and KNO₃, 3.0 mM K in the form of KH₂PO₄ and KNO₃, 1.5 mM Ca as Ca(NO₃)₂, 1.0 mM Mg as MgSO₄, 1.0 mM P as KH₂PO₄, and 0.5 mM Na as NaCl. Macronutrients were provided in the NH₄⁺-source solution as 5.0 mM N in the form of (NH₄)₂SO₄, 3.0 mM K as KH₂PO₄ and K₂SO₄, 1.5 mM Ca as CaCl₂ and CaSO₄, 1.0 mM Mg as MgSO₄, 1.0 mM P as KH₂PO₄, and 0.5 mM Na as NaCl. Micronutrients in NN or AN source solution were identical to those in the Mix-N source solution; and then kept in chambers (Figure 1A) with the following CO₂ levels: 280 μmol mol⁻¹ [pre-industrial revolution (i.e., 1840) concentration], 400 μmol mol⁻¹ (current level), and 550 μmol mol⁻¹ (projected concentration by the 2050 s) (IPCC, 2013). The temperature and humidity inside the chambers were automatically maintained to match those of the atmosphere outside (Figure 1B). During the night, the CO₂ gradients were held at concentrations 150 ± 1 μmol mol⁻¹ above daytime levels (Anderson et al., 2001).

A nitrification inhibitor (dicyandiamide, 1 mM) was added to the nutrition solutions to prevent microbial oxidation of NH₄⁺. The pH of the Hoagland's solution was adjusted daily to 5.5 using 0.1 mM NaOH for the plants treated with

NH₄⁺, or with 0.1 mM H₂SO₄ for those treated with NO₃⁻. The N concentrations were kept constant by replacing the media at 3-day intervals; aeration was provided continuously. We used three CO₂ treatments, with three replicates each in separate chambers (9 chambers in total), and deployed three N treatments for each species in each chamber. Ideally, each experiment should be repeated at least once in every chamber, for each of the planned treatments, to eliminate any intrinsic technical effect of each chamber on plant growth; this represented a potential small shortcoming of the current study in our facility.

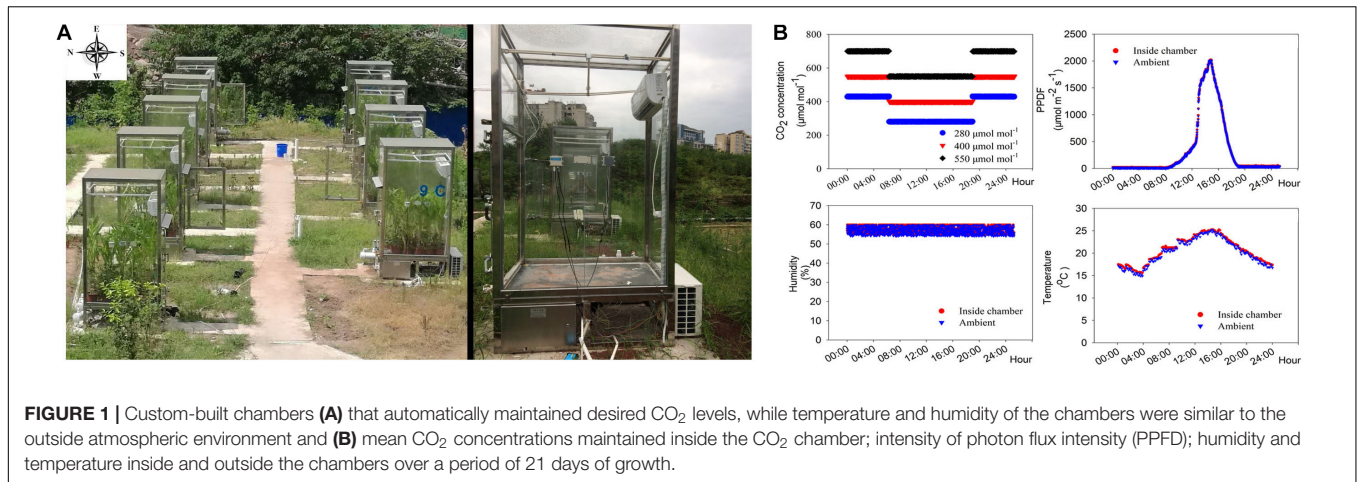
Experimental Field Chambers

The automatically CE facility consisted of a CO₂ control system (2543CN; Shengsen Corp., Qingdao, China; Supplementary Figures S1-1) and a CO₂ generator (12864; Shengsen Corp.; Supplementary Figure S1-2). The CO₂ generator comprised of several components, i.e., an electric connection point pressure meter (STC90C516RD; Shengsen Corp.), pressure sensors (13864; Shengsen Corp.), and Na₂CO₃ and H₂SO₄ feeding inlets (Supplementary Figures S1-5, 6), where the CO₂ was generated according to the following equation: Na₂CO₃+H₂SO₄=Na₂SO₄+H₂O+CO₂. The CO₂ generator was connected to the CO₂ control system to maintain the CO₂ concentration in the chambers within a desired set range; CO₂ was delivered through pipes into each chamber.

The chambers were built using toughened glass (10 mm thick, 99% transmittance) walls and roofs (Supplementary Figure S1-13). The floors were covered using a polyvinyl chloride (PVC) material (Supplementary Figure S1-7). Each chamber measured 1,500 × 1,000 × 2,000 mm (length × width × height). CO₂, temperature and humidity sensors were mounted on both the outer and inner surfaces of the walls (Supplementary Figures S1-8–10). The environmental control mechanism in this system operated automatically and regulated the internal CO₂ concentration (±2.5 μmol mol⁻¹), air temperature (±0.5°C) and humidity (±5%) (Figure 1B). The CO₂ control system sensed and assessed the chamber environmental data; these data were later used to regulate the CO₂ injection process and attaining the desired chamber CO₂ levels. When the CO₂ concentration in a chamber exceeded the set concentration, the air was filtered through 1.0 mol mol⁻¹ NaOH solution using a pump controlled by a mini-computer. When the humidity of a chamber exceeded the set concentration, the air was filtered through dry calcium carbonate using a separate pump controlled by the mini-computer.

Plant Sampling

The seedlings were sampled between 10:00 and 11:00 at the 21st day of the experiment. Plant organs were separated into two portions: the first was immersed in liquid-N and then stored at -80°C for later chemical analyses, and the second portion was oven-dried at 105°C for 20 min, and then at 75°C for at least 48 hours. The dried material was used later for different chemical analyses. Fresh leaf area was measured using a leaf area scanning device (Li-3000; Li-Cor Inc., Lincoln, NE, United States).



Gas-exchange Measurements

After 21 days of growth under different N source and CO₂ level conditions, we measured gas exchange and chlorophyll fluorescence simultaneously on the first fully developed leaves during the morning (09:00–11:00) using a Li-Cor 6400 infrared gas analyzer (Li-Cor 6400; Li-Cor Inc.). The leaf temperature during measurements was maintained at $25.0 \pm 0.5^\circ\text{C}$. Leaves were illuminated with a steady red and blue light source at a photosynthetic photon flux density (PPFD) of $1,500 \mu\text{mol m}^{-2} \text{s}^{-1}$ (Yong et al., 2000, 2010). The reference CO₂ concentrations in the cuvettes matched the treatment CO₂ concentrations to which samples had been previously subjected ($C_{\text{treatment}}$), i.e., 280 ± 2.5 , 400 ± 2.5 or $550 \pm 2.5 \mu\text{mol mol}^{-1}$. The vapor pressure deficit (Vpdl) was $1.1 \pm 0.05 \text{ kPa}$, and the relative humidity was in the range 55–65%. The gas exchange instrument was calibrated each day before the measurements and matched at least twice a day (between the curves). Data were recorded after sample acclimation in the cuvette for at least 15 min.

Two types of curves were plotted: net photosynthesis (A_n) vs. intercellular CO₂ concentrations (C_i , **Supplementary Figure S2**), and A_n vs. PPF. Simultaneous measurements of chlorophyll fluorescence and parameters for plotting the A/C_i curves were made on the same leaf using the Li-Cor 6400 infrared gas analyzer. Leaf temperature, PPF, Vpdl and relative humidity were maintained as indicated above. Prior to measurement, leaves were held in the cuvette at a reference CO₂ concentration of $C_{\text{treatment}}$ for at least 10 min. The reference CO₂ concentration was controlled across a series of $C_{\text{treatment}}$ values: 200, 150, 100, 50, 400, 600, 800, 1,000, 1,200, and $1,500 \mu\text{mol mol}^{-1}$. Data were collected after the prevailing CO₂ had reached a steady state (2–3 min).

Method for Determining Photosynthetic Parameters of C₃ and C₄ Plants

The parameters for the C₃ wheat plant photosynthesis model were calculated using the equations of Farquhar et al. (1980); Long and Bernacchi (2003), Gao et al. (2018), and Wang et al. (2019).

According to the photosynthesis model that we used for C₄ maize plants (von Caemmerer and Farquhar, 1999), the rates of phosphoenolpyruvate (PEP) and Rubisco carboxylation (V_p and V_c , respectively) are the major determinants of the net CO₂ assimilation rate. The Rubisco carboxylation rate (V_{cmax}), the maximal rate of PEP carboxylation (V_{pmax}), maximum RuBP-regeneration rate (J_{max}) and CO₂ concentration in the bundle sheath (C_s) for maize were calculated using the following equations. The photosynthetic rate was expressed mathematically as:

$$A = V_p - R_m - L \quad (1)$$

and

$$A = V_c - 0.5V_0 - R_d \quad (2)$$

where R_m is the mitochondrial respiration of the mesophyll cells, L is the rate of CO₂ leakage from the bundle sheath into the mesophyll, and R_d is the mitochondrial respiration rate in the light.

$$L = g_{bs} \times (C_s - C_m) \quad (3)$$

$$C_m = C_i - \frac{A}{g_i} \quad (4)$$

where g_{bs} is the bundle sheath conductance for CO₂, g_i is the mesophyll conductance for CO₂, C_s is the CO₂ concentration in the bundle sheath, and C_m is the CO₂ concentration in the mesophyll cells. V_0 is the rate of Rubisco oxygenation:

$$V_0 = \frac{2\gamma^* O}{C_s} \times V_c \quad (5)$$

where γ^* is one half of the reciprocal of Rubisco specificity ($S_{c/o}$), and O is the oxygen concentration in the bundle sheath cells, which matches the oxygen concentration in the mesophyll cells. By fitting equation (3) to equation (1), and equation (5) to equation (2), we obtained the following expressions:

$$A = V_p - R_m - g_{bs} \times (C_s - C_m) \quad (6)$$

and

$$A = V_c \times \left(1 - \frac{\gamma^* O}{C_s}\right) - R_d \quad (7)$$

V_p and V_c depend on V_{cmax} , V_{pmax} , J_{max} , the Michaelis constants for O₂ and CO₂ (K_o , K_c and K_p), and the relative specificity of Rubisco ($S_{c/o}$).

To calculate V_{cmax} and V_{pmax} , we used the enzyme-limited expressions of V_p and V_c :

$$V_p = \frac{C_m V_{pmax}}{C_m + K_p} \quad (8)$$

$$V_c = \frac{C_s V_{cmax}}{C_s + K_p \left(1 + \frac{O}{K_o}\right)} \quad (9)$$

By fitting equation (8) to equation (6), and equation (9) to equation (7), we obtained the following expressions:

$$A = \frac{C_m V_{pmax}}{C_m + K_p} - R_m - g_{bs} \times (C_s - C_m) \quad (10)$$

and

$$A = \frac{C_s V_{cmax}}{C_s + K_c \left(1 + \frac{O}{K_o}\right)} \times \left(1 - \frac{\gamma^* O}{C_s}\right) - R_d \quad (11)$$

In equations (4), (10) and (11), g_i , g_{bs} , R_m , K_p , K_c , K_o , O , R_d and γ^* were constant parameters at a given temperature [as described by von Caemmerer and Farquhar (1999)], A and C_i were measured values, and C_m , C_s , V_{cmax} and V_{pmax} were unknowns. Two pairs of (A , C_i) (with C_i limited to 40–80 $\mu\text{mol mol}^{-1}$) were then inserted into two sets of equations (5), (8) and (9), following which we obtained six equations and six unknowns (V_{cmax} , V_{pmax} , C_s1 , C_s2 , C_m1 and C_m2) using the Matlab software (MathWorks, Natick, MA, United States).

To calculate J_{max} , we used the electron transport limited expressions of V_p and V_c :

$$V_p = \frac{xJ_t}{2} \quad (12)$$

$$V_c = \frac{(1-x)J_t}{3 \left(1 + \frac{7\gamma^* O}{3C_s}\right)} \quad (13)$$

where x is a partitioning factor of electron transport, and J_t is the electron transport rate, given by:

$$J_t = \frac{I_2 + J_{max} - \sqrt{(I_2 + J_{max})^2 - 4\theta I_2 J_{max}}}{2\theta} \quad (14)$$

where I_2 is the total absorbed irradiance, which is a function of the incident irradiance I , and θ is an empirical curvature factor.

By fitting equation (11) to equation (6), and equation (12) to equation (7), we obtained:

$$A = \frac{xJ_t}{2} - R_m - g_{bs} \times (C_s - C_m) \quad (15)$$

and

$$A = \frac{(1-x)J_t}{3 \left(1 + \frac{7\gamma^* O}{3C_s}\right)} - R_d \quad (16)$$

C_m was obtained from equation (4). In equations (15) and (16), x and γ^* are constants at a given temperature, A , C_m and I (PPFD) are known values, and J_{max} and C_s are unknown entities. With two equations and two unknowns, and incorporating the single values of A and I (PPFD), we obtained the values for J_{max} and C_s .

Chlorophyll Fluorescence Measurements

Light adapted chlorophyll fluorescence was measured with a Li-Cor 6400 infrared gas analyzer while simultaneously measuring gas exchange, as described above. Steady-state fluorescence (F_s) was measured under actinic light. A saturating light pulse ($\sim 8,000 \mu\text{mol photons m}^{-2} \text{s}^{-1}$) was applied for 0.7 s to obtain the maximum fluorescence (F_m'). After removing the actinic light and applying 3 s of far-red light, the minimal fluorescence of the light-adapted state (F_o') was obtained. The quantum efficiency of PSII (Φ_{PSII}) and J_t were calculated using equations (17) and (18), respectively, following Genty et al. (1989) and Li et al. (2009):

$$\Phi_{PSII} = \frac{F_m' - F_s}{F_m'} \quad (17)$$

$$J_t = \frac{F_m' - F_s}{F_m'} \times \text{PPFD} \times 0.85 \times 0.5 \quad (18)$$

The central portion of the same leaf ($\sim 70\%$ leaf area) was chosen for measurement of dark-adapted and light-adapted chlorophyll fluorescence parameters using a Fluor imager (CF Imager; Technologia Ltd., Colchester, United Kingdom). The minimum and maximum chlorophyll fluorescence (F_o and F_m , respectively) values were determined after full dark adaptation for at least 30 min. F_s , F_m' , and F_o' were obtained as described above. The maximum quantum efficiency of PSII (F_v/F_m) was calculated using equation (32) of Genty et al. (1989):

$$F_v/F_m = \frac{F_m - F_o}{F_m} \quad (19)$$

Photochemical quenching (qL) was calculated using equation (20) and non-photochemical quenching (NPQ) was calculated using equation (21), following Kramer et al. (2004).

$$qL = \frac{F_o'}{F_s} \times \frac{F_m' - F_s}{F_m' - F_o'} \quad (20)$$

$$\text{NPQ} = \frac{F_m - F_m'}{F_m'} \quad (21)$$

Calculating Electron Flux to the Photosynthetic Carbon Reduction Cycle [Je(PCR)], and Electron Flux to the Photorespiratory Carbon Oxidation Cycle [Je(PCO)]

The J_t in the photosynthetic carbon reduction and photorespiratory carbon oxidation cycles were expressed as

follows (Zhou et al., 2004):

$$Je(PCR) = 4 \times v_c = 4 \times \frac{A + R_d}{1 - \frac{\Gamma^*}{C_i}} \quad (22)$$

$$Je(PCO) = 4 \times v_o \quad (23)$$

Determination of Free NH₄⁺ and Soluble Sugar Concentrations

The free NH₄⁺ in plant tissues was determined according to Balkos et al. (2010) with some modifications. Briefly, plant tissues were desorbed in 10 mM CaSO₄ for 5 min, and then rinsed with deionized water to remove any extracellular NH₄⁺. Approximately 0.5 g of fresh material was homogenized with liquid nitrogen; NH₄⁺ was then extracted in 5 ml of 10 mM formic acid. Supernatants were collected after centrifugation at 10,000 g (4°C) for 15 min, transferred to 5-ml polypropylene tubes after filtration through 0.45-μm organic ultra-filtration membranes, and re-centrifuged at 50,000 g (4°C) for 10 min. An *O*-phthalaldehyde (OPA) reagent was prepared by combining 200 mM potassium phosphate buffer (equimolar amounts of potassium dihydrogen phosphate and potassium monohydrogen phosphate), 3.75 mM OPA, and 2 mM 2-mercaptoethanol (v/v/v = 1:1:1). Prior to adding 2-mercaptoethanol, the pH was adjusted to 7.0 using 1 M NaOH, and the solution was then filtered through two layers of filter paper. A 10-μl aliquot of tissue extract was mixed with 3 ml of OPA reagent. The color was developed in darkness at 25°C for 30 min before carrying out absorbance measurements at 410 nm using a spectrophotometer (model UV-2401, Shimadzu Corp., Kyoto, Japan).

Soluble sugar concentrations were measured following the method of Wang et al. (2016a). Dry powdered shoot and root samples (0.5 g) were extracted in 80% (v/v) ethanol at 80°C for 30 min. The extracts were later centrifuged at 3000 g for 10 min and the supernatants were collected. This extraction procedure was repeated three times to ensure all soluble sugars were extracted. The supernatants were evaporated on china dishes in a hot water bath. Residues were then re-dissolved in 1-3 ml of distilled water and filtered through 0.4-μm film to assay soluble sugars. Concentrations of soluble sugar were measured using the anthrone method. Anthrone sulfuric acid (5 ml) solution (75% v/v) was added to 0.1 ml of supernatant and heated to 90°C for 15 min. Absorbance at 620 nm was measured using a spectrophotometer (model UV-2401, Shimadzu Corp., Kyoto, Japan).

Statistical Analysis

We found significant effects of N forms (Mix-N, NN, AN) and CO₂ levels on the measured parameters in wheat and maize using the two-way ANOVA ($P < 0.05$, $n = 3$). Significant pairwise differences between means were identified with Dunnett's multiple comparisons test ($P < 0.05$). The proportion of variation (%) explainable by each factor was estimated as the total sums of squares. Calculations were performed with SPSS software (SPSS, Inc., Chicago, United States). Graphs were plotted

using SigmaPlot 10.0 software (Systat Software, Inc., Chicago, IL, United States).

RESULTS

Dry Biomass, Leaf Area and Free NH₄⁺

Compared with the Mix-N treatment, AN significantly reduced the shoot and root biomass of both wheat and maize plants (Figure 2). However, with increasing CO₂ concentration, wheat shoot and root biomass increased significantly, although these biomass parameters did not differ significantly according to CO₂ levels in maize. Shoot biomass in wheat under AN was reduced by 38%, 27%, and 14% at CO₂ concentrations of 280, 400 and 550 μmol mol⁻¹, respectively (in comparison with the Mix-N treatment). The decreases were larger in maize (46%, 44% and 44% at CO₂ concentrations of 280, 400, or 550 μmol mol⁻¹, respectively) (Figure 2). The AN treatment reduced the total leaf area, where the reduction was again greater in maize than in wheat. With increasing CO₂ concentrations, the total foliage area of wheat increased significantly, but this was not the case for maize. Free NH₄⁺ concentrations did not differ significantly in either species between the Mix-N and NN treatments with increasing CO₂ concentration (Figure 2) whereas, in comparison with the other two treatments, the AN increased free NH₄⁺ in shoots and roots. The concentration of free NH₄⁺ decreased significantly with increasing CO₂ concentration in wheat, but not in maize.

Only the N form had significant effects on maize shoot dry biomass; in wheat, the N form, CO₂ level, and their interaction significantly affected shoot biomass (Table 1). Changes in CO₂ levels caused a higher proportion of the variance in wheat shoot dry biomass than did changes in N form. Total leaf area in the two species was significantly affected by both N form and CO₂ level. N form explained a larger proportion of the variance in total leaf area in both species. Alterations in CO₂ levels explained a much greater proportion of the variance in total leaf area variation in wheat (38%) than in maize (0.5%). In both species, the quantity of free NH₄⁺ in shoots and roots differed significantly according to the form of N supplied. Interestingly, the CO₂ level had significant effects on free NH₄⁺ in tissues of wheat, but not in maize.

Photosynthesis and Its Related Parameters

Compared with Mix-N and NN, AN treatment reduced the net photosynthetic rate (P_n) of both maize and wheat, although the effect was greater in the former species (Figure 3). The P_n of wheat plants growing under 550 μmol CO₂ mol⁻¹ was significantly higher than that of plants grown under 280 and 400 μmol CO₂ mol⁻¹. Conversely, the P_n of maize plants under AN did not differ significantly according to the CO₂ level. On day 21 of the experiment, the P_n of maize under AN was reduced in comparison with those under the Mix-N treatment, by 34%, 32% and 32% at CO₂ concentrations of 280, 400, and 550 μmol mol⁻¹, respectively. The respective reductions in wheat were 30%, 27% and 19%.

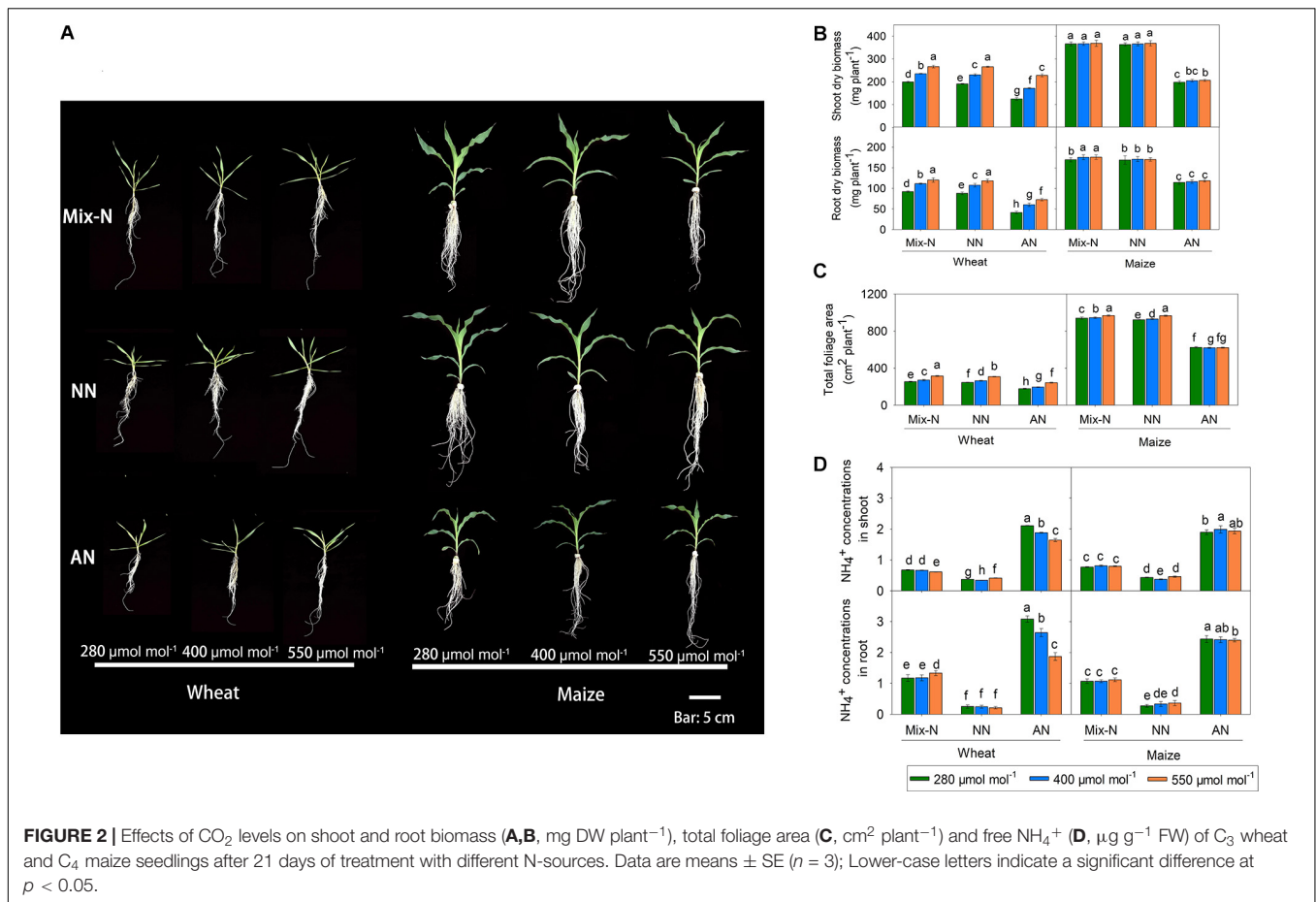


TABLE 1 | F-values in two-way ANOVA analysis of biomass, total foliage area and free NH₄⁺ in newly expanded leaves of C₃ wheat and C₄ maize seedlings after 21 days of treatment with different N-sources.

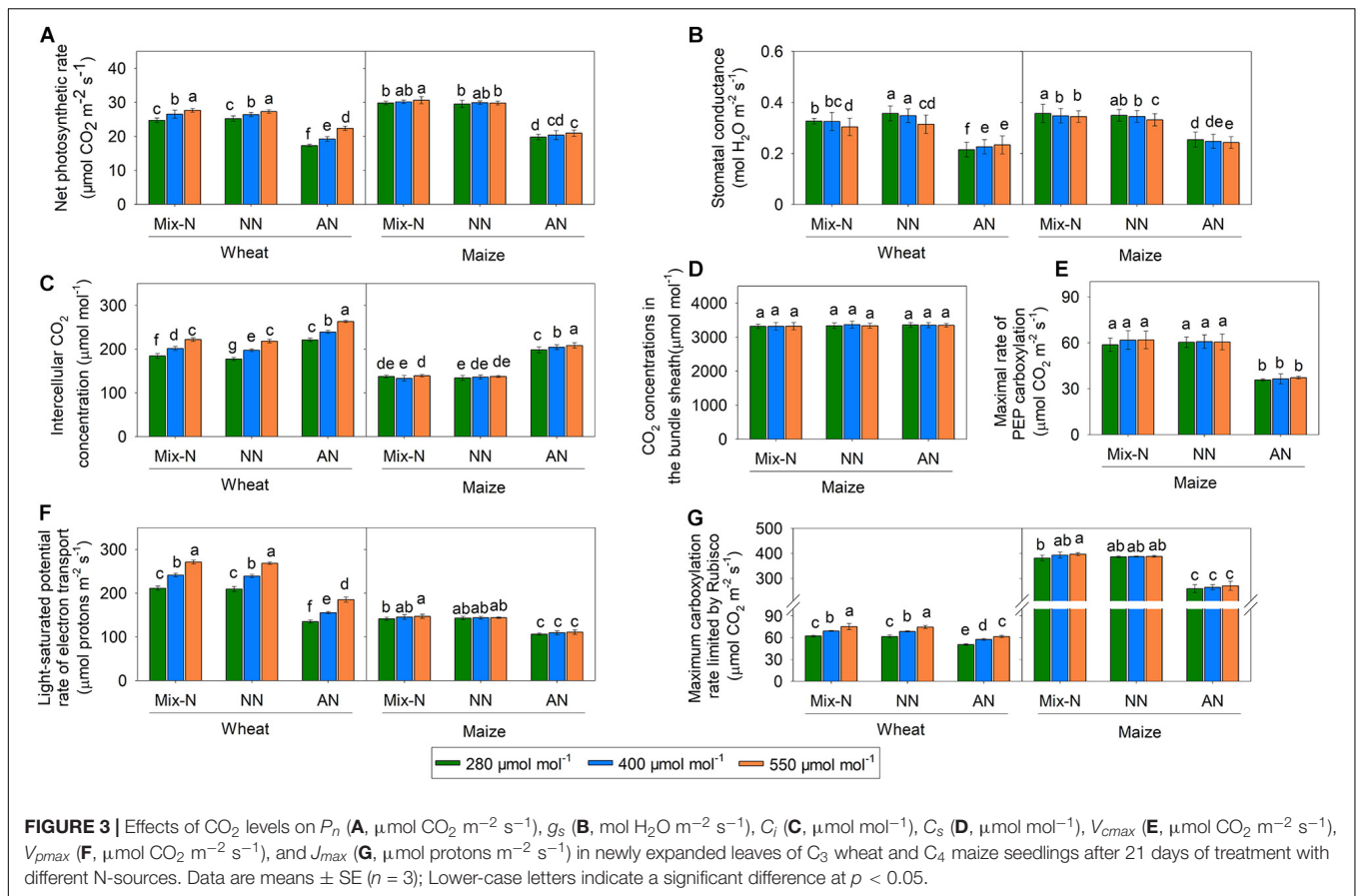
Species	N-form	CO ₂ level	Shoot dry weight		Root dry weight		Total foliage area		Free NH ₄ ⁺ in shoot		Free NH ₄ ⁺ in root	
Species	Source	df	Squares sum (x10 ³)	F-value	Squares sum (x10 ²)	F-value	Squares sum (x10 ³)	F-value	Squares sum	F-value (x10 ²)	Squares sum	F-value (x10 ²)
Wheat	N	2	38.8(38.1)	2758**	279.8(76.5)	1822**	61(61.2)	1824**	23.09(97.1)	337.6**	47.6(91.0)	115.0**
	CO ₂	2	60.5(59.4)	4302**	82.8(22.6)	539**	38(38.1)	1134**	0.24(1.0)	3.5**	1.2(5.3)	2.9**
	N × CO ₂	4	2.3(2.3)	83**	0.3(0.1)	1 ns	0 (0.0)	1 ns	0.40(1.9)	3.3**	3.4(15.1)	4.1**
	Error	40	0.3(0.3)		3.1(0.8)		1(0.7)		0.01(0.1)		0.1(0.4)	
Maize	N	2	321.2(99.3)	3445.6**	372.4(97.9)	1279**	1258(99.2)	42843**	22.50(99.3)	48.0**	40.0(99.6)	71.9**
	CO ₂	2	0.3(0.08)	2.7 ns	1.6(0.4)	5**	6(0.5)	197**	0.01(0.0)	0.0 ns	0.0(0.0)	0.0
	N × CO ₂	4	0.1(0.03)	0.5 ns	0.6(0.1)	1 ns	4(0.3)	61**	0.04(0.2)	0.1**	0.0(0.2)	0.0
	Error	40	1.9(0.58)		5.8(1.5)		1(0.0)		0.09(0.4)		0.1(0.5)	

N refers to the three nitrogen-forms effect; CO₂ refers to the three CO₂ levels effect; N × CO₂ refers to nitrogen-form × CO₂ levels interaction effects. Values in brackets following the sum of squares for variables indicate the percentage (%) of given variation to total variation. ** indicate significant at 0.01 level, respectively. df refers to the degree of freedom. ns means no significant difference.

The g_s values did not differ significantly by CO₂ concentration, but were significantly reduced by AN treatment compared with the other two treatments, in both species (Figure 3). C_i increased significantly with increasing CO₂ concentration in wheat, but not in maize. The AN treatment significantly increased C_i in both species in comparison with the other two treatments. On day 21 of the experiment, we found no significant differences

in C_s according to either the treatment or CO₂ concentration. V_{pmax} did not vary significantly by CO₂ concentration, but was significantly reduced under AN in comparison with the other two treatments.

The V_{cmax} and J_{max} of wheat increased significantly with increasing CO₂ concentration within the same level of the N form factor, but this was not the case for maize (Figure 3).



In comparison with the other two treatments, AN reduced V_{cmax} and J_{max} in both species. The reduction in V_{cmax} associated with AN was larger in maize than in wheat, while the reduction in J_{max} was smaller in maize than in wheat. On day 21 of the experiment, AN reduced V_{cmax} in maize in comparison with Mix-N, by 32%, 33% and 32% at CO₂ concentrations of 280, 400, and 550 $\mu\text{mol mol}^{-1}$, respectively. The respective reductions in wheat were 19%, 17%, and 18%. Moreover, AN reduced the J_{max} of maize in comparison with Mix-N, by 25%, 25%, and 24% at CO₂ concentrations of 280, 400, and 550 $\mu\text{mol mol}^{-1}$, respectively. The respective reductions in wheat were 36%, 36%, and 32%.

The P_n , g_s , C_i , V_{cmax} and J_{max} varied significantly according to both the N treatment type and the CO₂ level. The N form accounted for a larger proportion of the variance in these parameters in both species (Table 2). The effect of CO₂ level was much greater in wheat than in maize. The V_{pmax} of maize was significantly affected only by the N form. The C_s in maize was not affected by the N form, CO₂ level, or their interaction, nor by the interaction between pH and the N form.

Electron Transport Parameters

Under Mix-N and NN, the F_v/F_m , Φ_{PSII} and qL values of the two species did not vary significantly across different CO₂ concentration (Figures 4A–C). The values of these parameters decreased with increasing CO₂ concentration in maize plants

under AN, but increased in wheat plants as CO₂ concentrations rose. NPQ increased significantly under AN in comparison with the other treatments, but did not differ significantly by CO₂ level (Figure 4D). The F_v/F_m , Φ_{PSII} and qL values of wheat varied significantly by both N form and CO₂ concentration, as observed for Φ_{PSII} and qL in maize (but not for F_v/F_m). N form explained a larger proportion of the variance in these parameters in both species than CO₂ concentration (Table 3). CO₂ level accounted for a larger proportion of the variance in electron transport in wheat (8.9% for F_v/F_m , 5.1% for Φ_{PSII} and 5.5% for qL) than in maize (0.0% for F_v/F_m , 0.5% for Φ_{PSII} and 0.4% for qL).

Under Mix-N and NN, the values of J_t for both species did not differ significantly across different CO₂ concentration (Figure 5A). However, while the values of J_t for wheat plants under AN increased significantly with increasing CO₂ concentration, this was not the case for maize. On day 21 of the experiment, AN reduced the J_t values to below those of plants under Mix-N, by 31%, 32% and 32% in maize at CO₂ concentrations of 280, 400, or 550 $\mu\text{mol mol}^{-1}$, respectively. The respective reductions in wheat were 38%, 30%, and 21%. The $Je(PCR)$ values of wheat were higher under CO₂ concentrations of 400 and 550 $\mu\text{mol mol}^{-1}$ than under a concentration of 280 $\mu\text{mol mol}^{-1}$. CO₂ level had no significant effect on the $Je(PCR)$ values of maize (Figure 5B). In comparison with the other treatments, AN significantly reduced $Je(PCR)$ in both species. Under AN, the $Je(PCR)$ values of wheat increased

TABLE 2 | F-values in two-way ANOVA analysis of P_n , g_s , C_i , C_s , V_{cmax} , V_{pmax} , and J_{max} in newly expanded leaves of C₃ wheat and C₄ maize seedlings after 21 days of treatment with different N-sources.

Species	N-form	CO ₂ level	P_n	g_s	C_i	C_s	V_{cmax}	V_{pmax}	J_{max}
Species	Source	df	Squares sum ($\times 10^3$)	F-value	Squares sum ($\times 10^3$)	F-value	Squares sum ($\times 10^3$)	Squares sum ($\times 10^2$)	Squares sum ($\times 10^3$)
Wheat	N	2	532(80.7)	1217**	205.0(57.7)	2758**	1.75(53.7)	273**	80.1(73.0)
	CO ₂	2	102(15.4)	232**	145.3(40.9)	4302**	1.38(42.1)	214**	28.7(26.1)
	N \times CO ₂	4	17(2.5)	18*	0.4(0.1)	83**	0.01(0.3)	1 ns	0.2(0.2)
	Error	40	9(1.3)	4(2.7)	4.7(1.3)	0.13(3.9)			0.7(0.6)
Maize	N	2	1108(98.3)	1647**	546.3(98.4)	2396**	184.7(97.0)	826**	14.9(94.9)
	CO ₂	2	5(0.4)	7**	2.4(0.4)	10**	0.9(0.5)	4*	0.1(0.9)
	N \times CO ₂	4	1(0.1)	1 ns	2.0(0.4)	4**	0.3(0.2)	1 ns	0.0(0.3)
	Error	40	13(1.2)	2(1.7)	4.6(0.8)	2987(95.3)	4.5(2.3)	5.5(7.3)	0.6(4.0)

N refers to the three nitrogen-forms effect; CO₂ refers to the three CO₂ levels effect; N \times CO₂ refers to nitrogen-form \times CO₂ levels interaction effects. Values in brackets following the sum of squares for variables indicate the percentage (%) of given variation to total variation. * and ** indicate significant at 0.05 and 0.01 level, respectively. df refers to the degree of freedom. ns means no significant difference.

significantly with increasing CO₂ concentration, but this was not the case for maize. When compared to other N form treatments, AN significantly reduced $Je(PCO)$ in both species (**Figure 5C**) on day 21 of the experiment. The $Je(PCR)/Je(PCO)$ ratio increased significantly with increasing CO₂ concentration in wheat. The ratio in maize was unaffected by either CO₂ level or N form (**Figure 5D**).

J_t , $Je(PCR)$, $Je(PCO)$ and the $Je(PCR)/Je(PCO)$ ratio were significantly affected by N form and CO₂ level in both species. N form explained a larger proportion of the variance in these parameters in both species (**Table 4**). In wheat, 40% of the variance in the $Je(PCR)/Je(PCO)$ ratio could be attributed to CO₂ level, but this factor accounted for only 2.9% of the variance in maize (**Table 4**).

Soluble Sugars

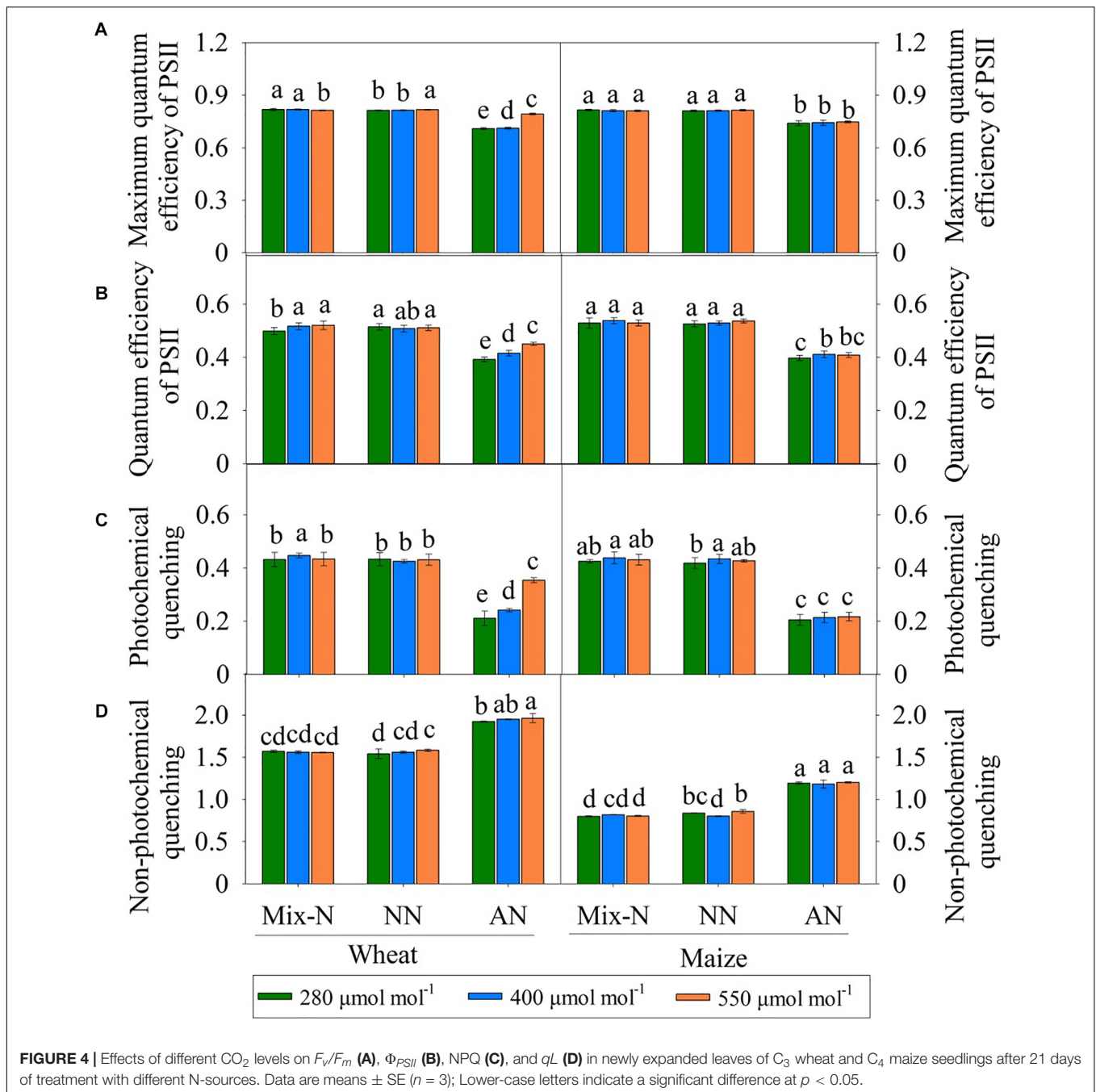
In comparison with the other N form treatments, AN markedly reduced the soluble sugar concentration in both species. Soluble sugar levels in the shoots and roots of wheat increased with increasing CO₂ concentration, but this was not the case in maize (**Figure 6**).

DISCUSSION

Increased Atmospheric CO₂ Concentrations Offset NH₄⁺-Linked Stress in C₃ Wheat but Not in C₄ Maize

Unlike field or pot experiments, hydroponic experiments remove any potential complex interaction between ions and soil particles that might affect nutrient availability, and thus plant growth and development (Conn et al., 2013; Nguyen et al., 2016). We harnessed the hydroponic approach to study the responses of C₃ wheat and C₄ maize to different N forms and three levels of CO₂ concentrations. In previous studies, the most obvious effect of AN was reduced biomass production (Britto and Kronzucker, 2002; Li et al., 2011; Wang et al., 2016b, 2019). In the present study, the Mix-N and NO₃⁻-fed C₃ wheat plants produced more dry biomass when the corresponding C_a concentration was increased, but this was not the case for C₄ maize, corroborating the findings of Leakey et al. (2006). When C_a was low, the leaf-free NH₄⁺ content was highest in C₄ maize with NH₄⁺ as the sole N source (**Figure 2**); concomitantly under these conditions, we recorded the lowest P_n values for maize (**Figure 3**).

In C₃ wheat, AN-induced photosynthetic inhibition was ameliorated by increasing the C_a concentration, but this effect was insignificant in C₄ maize (**Figure 3**). Franks et al. (2013) found that change in C_a concentration changes the rates of carboxylation by Rubisco (in C₃ plants) and PEP carboxylase (in C₄ plants); each of these enzymes has a crucial limiting step in the photosynthetic pathway. An initial increase in P_n (less pronounced in C₄ plants) at or above the ambient C_a concentration occurs because of the unique CO₂-concentrating mechanism associated with C₄ photosynthesis (Ghannoum et al., 1997; von Caemmerer and Farquhar, 1999). In our study, we



further explored (i) the potential limiting factors of P_n when C₃ and C₄ plants were grown under condition of NH₄⁺-N nutrition, and (ii) the way in which changes in C_a concentration affected the potential NH₄⁺ tolerance of C₃ and C₄ plants.

Impaired Electron Transfer Associated With NH₄⁺ Inhibited Photosynthesis

Under atmospheric CO₂ conditions, the carboxylation ability of Rubisco is the key factor limiting C₃ photosynthesis (Li et al., 2009; Carmo-Silva et al., 2015). V_{cmax} , which represents

the apparent Rubisco activity *in vivo* (Long and Bernacchi, 2003), increases with increasing CO₂ concentration (Jordan and Ogren, 1984). We found that both wheat and maize plants had lower g_s and V_{cmax} values under AN than under the other two N treatments, but C_i values were elevated under AN (Figure 3). Early CO₂ enrichment experiments using crops and tree saplings demonstrated that g_s was generally reduced by elevated CO₂ concentrations; we noted a similar phenomenon in wheat (Figure 3) (Yong et al., 1997; Medlyn et al., 2001). In contrast, the C_i and C_s of maize changed less with increases in C_a , regardless of the type of N nutrition. Li et al. (2015) suggested

TABLE 3 | *F*-values in two-way ANOVA analysis of *F_v/F_m*, Φ_{PSII} , NPQ and *qL* in newly expanded leaves of C₃ wheat and C₄ maize seedlings after 21 days of treatment with different N-sources.

Species	Source	df	<i>F_v/F_m</i>		Φ_{PSII}		NPQ		<i>qL</i>	
			Squares sum ($\times 10^{-3}$)	<i>F</i> -value	Squares sum ($\times 10^{-3}$)	<i>F</i> -value	Squares sum ($\times 10^{-3}$)	<i>F</i> -value	Squares sum ($\times 10^{-3}$)	<i>F</i> -value
Wheat	N	2	73(72.3)	11450**	102(86.4)	510**	1768(98.1)	1485**	326(81.7)	1753**
	CO ₂	2	9(8.9)	1369**	6(5.1)	29**	5(0.2)	4*	22(5.5)	117**
	N \times CO ₂	4	19(18.8)	1478**	6(5.1)	15**	6(0.5)	3*	47(11.8)	127**
	Error	40	0(0.0)		4(3.4)		24(0.9)		4(1.0)	
Maize	N	2	57(96.6)	478**	189(96.7)	1013**	1671(98.4)	2249**	564(98.8)	2277**
	CO ₂	2	0(0.0)	0 ns	1(0.5)	4*	4(0.2)	5*	2(0.4)	6**
	N \times CO ₂	4	0(0.0)	1 ns	1(0.5)	2 ns	8(0.5)	6**	0(0.0)	1 ns
	Error	40	2(3.4)		4(2.1)		15(0.9)		5(0.9)	

N refers to the three nitrogen-forms effect; CO₂ refers to the three CO₂ levels effect; N \times CO₂ refers to nitrogen-form \times CO₂ levels interaction effects. Values in brackets following the sum of squares for variables indicate the percentage (%) of given variation to total variation. * and ** indicate significant at 0.05 and 0.01 level, respectively. *df* refers to the degree of freedom. ns means no significant difference.

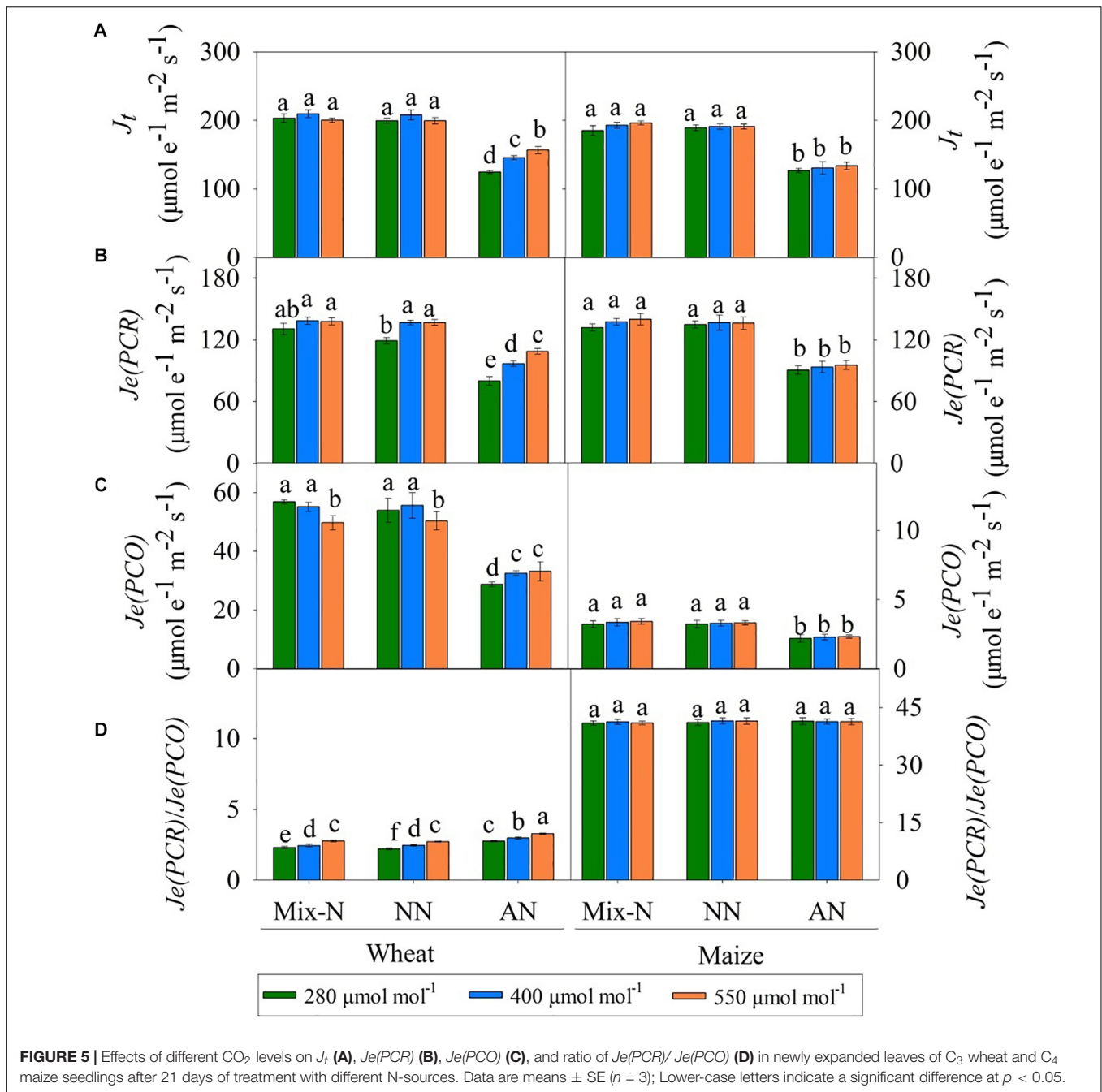
that the increases in *C_i* may result from decreases in the rate of the photosynthetic dark CO₂ reduction when *g_s* is reduced in C₃ plants.

Under ambient conditions, 44% of the absorbed light at peak PPFD was used for photosynthetic electron transport (25% for CO₂ fixation, 19% for photorespiration), and the remaining 56% was dissipated by chlorophyll fluorescence and thermal energy generation (Demmig-Adams and Adams, 1992). The balance between photosynthetic electron harvesting and transport within the chloroplasts is important for CO₂ assimilation based on the Calvin cycle (Demmig-Adams et al., 1989; Fryer et al., 1998; Shikanai, 2011). We found that *F_v/F_m*, Φ_{PSII} , *qL* and *J_t* were reduced under conditions of NH₄⁺ nutrition (Figures 4A–C, 5A), indicating that the energy available for CO₂ assimilation was limited. Similar responses under conditions of NH₄⁺ nutrition were reported by Johnson et al. (2011), where the photosynthetic electron transport chain was interrupted on the PSII side. The oxygen-evolving complex of PSII may be a direct target of NH₄⁺, causing a marked decline in photosynthesis (Drath et al., 2008). We found significant reductions in *J_{max}*, Φ_{PSII} and *J_t* for both wheat and maize (Figures 3, 4B, 5A); the reductions for maize were especially marked, and led to deficiencies in NADPH and ATP availability for CO₂ assimilation (Gao et al., 2018). Cousins and Bloom (2003) suggested that NO₃⁻ assimilation increases linear electron transfer and alleviates the photosynthetic ATP limitation in maize. In NH₄⁺-fed plants, the inadequate energy supply for CO₂ carboxylation may be a result of interruptions in the electron transport chain (Wang et al., 2019). With an impaired PSII, plants have a reduced capacity to dissipate excitation energy through *qL*, resulting in a surplus of light energy (Kim and Apel, 2013). We found that NPQ increased in both species (Figure 4D) via a process involving the scavenging of excess light energy through heat dissipation under conditions of NH₄⁺ nutrition. This finding was consistent with a previous report showing that plants can dissipate excess excitation energy in the form of heat through NPQ when they encountered abiotic stresses (Demmig-Adams and Adams, 1992).

Higher C_a Enhanced CO₂ Assimilation, Which Provided Additional C Skeletons for NH₄⁺ Assimilation in C₃ Plants

Under AN, the *J_{max}*, Φ_{PSII} and *J_t* values of wheat increased with increasing CO₂ concentration (Figures 3, 4B, 5A), indicating that the interruption in electron transport can be offset by higher CO₂ concentration; these parameters did not differ significantly for maize grown under different CO₂ levels. At low atmospheric CO₂ levels, Rubisco utilizes both CO₂ and O₂ (Edwards et al., 2010). The process of uptaking O₂ leads to photorespiration, resulting in net losses of $\leq 40\%$ of photosynthetic carbon under present day CO₂ levels of 400 $\mu\text{mol mol}^{-1}$ (Andrews and Lorimer, 1978; Sage, 2004; Bloom, 2015). C₄ photosynthesis suppresses photorespiration by concentrating CO₂ internally (Andrews and Lorimer, 1978; Ehleringer et al., 1991). Conversely, higher C_a increases the CO₂ assimilation of C₃ plants and thereby inhibiting photorespiration; C₄ plants do not respond in this way (Andrews and Lorimer, 1978). We found that the *C_i* and *C_c* values of wheat under AN increased significantly with increased C_a, leading to increases in *Je(PCR)*, whereas *Je(PCO)* did not change significantly (Figure 5D). As a result, the *Je(PCR)/Je(PCO)* ratio increased with increasing CO₂ concentration under AN (Figure 5C). These findings indicated that the electron flux to CO₂ assimilation was increased at higher CO₂ concentrations, which may compensate for the decrease in electron transport ability seen under AN, thereby sustaining carbon assimilation. In maize, there were no significant differences in *C_i*, *C_c* or *Je(PCR)/Je(PCO)* by CO₂ level on day 21 of the experiment (Figures 2, 5D).

Bloom et al. (2010) and Bloom (2015) found that (i) elevated CO₂ inhibits nitrite (NO₂⁻) transport into chloroplasts, (ii) the chloroplast stroma compete for reduced ferredoxin (Fdr), and (iii) elevated CO₂ levels decrease photorespiration, thereby inhibiting shoot NO₃⁻ assimilation in C₃ plants under elevated CO₂ concentrations. In contrast, the first carboxylation reaction in the C₄ carbon fixation pathway generates ample quantities of malate and NADH in the cytoplasm of mesophyll cells.



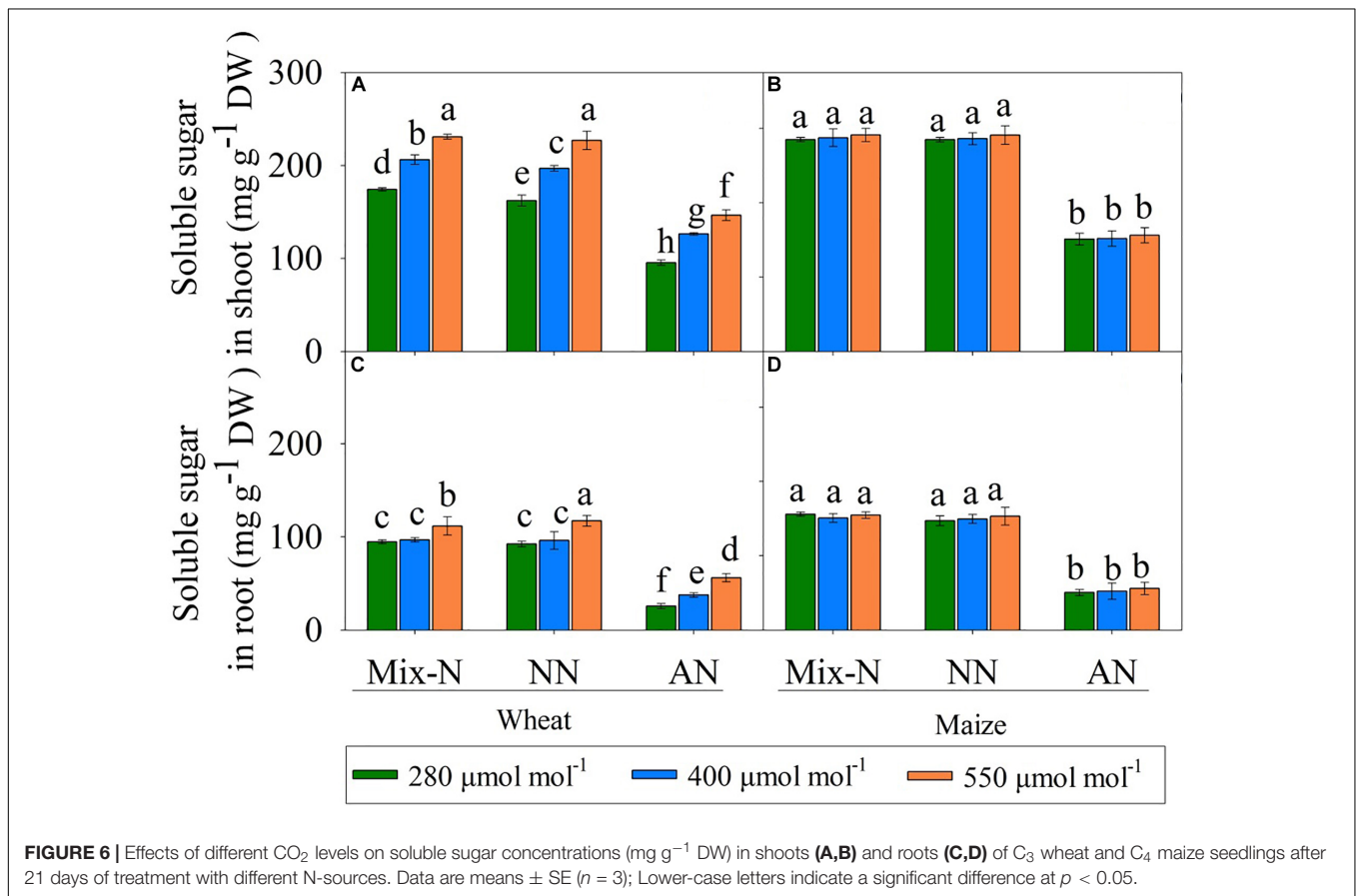
This explains adequately the CO₂-independent shoot NO₃⁻ assimilation in C₄ plants (Bloom et al., 2010). However, since N assimilation occurs rapidly when NH₄⁺ is the sole source of N nutrition, an adequate C skeleton supply for NH₄⁺ assimilation is required to facilitate general physiological homeostasis under elevated NH₄⁺ concentrations (Ariz et al., 2013). Therefore, the carbohydrate status of plant tissues has an important role in the transition and adaptation to AN nutrition. A shortage of carbon assimilation for NH₄⁺ form has been associated with a reduced level of soluble sugars in NH₄⁺-grown plants (Setien et al., 2013). We found

a significant decrease in the soluble sugar concentration in both species, especially in roots, under AN and ambient CO₂ conditions (Figure 6). With increasing C_a, an increase in soluble sugar concentration and a decrease in free NH₄⁺ concentration occurred in wheat, possibly because of an increase in CO₂ photosynthetic capacity (Ariz et al., 2010, 2013). Therefore, in wheat, an increased P_n under AN, which was driven by elevated C_a levels, increased the supply of carbon skeleton for NH₄⁺ assimilation, which in turn reduced the NH₄⁺ concentrations and thereby ameliorating the NH₄⁺ stress.

TABLE 4 | *F*-values in two-way ANOVA analysis of *J_t*, *Je(PCR)*, *Je(PCO)*, and ratio of *Je(PCR)/Je(PCO)* in newly expanded leaves of C₃ wheat and C₄ maize seedlings after 21 days of treatment with different N-sources.

Species	Source	df	<i>J_t</i>		<i>Je(PCR)</i>		<i>Je(PCO)</i>		<i>Je(PCR)/Je(PCO)</i>	
			Squares sum (×10 ³)	<i>F</i> -value	Squares sum (×10 ³)	<i>F</i> -value	Squares sum	<i>F</i> -value	Squares sum	<i>F</i> -value
Wheat	N	2	44.5(90.5)	931**	17.6 (79.7)	719**	5885 (90.1)	363.3**	3.29(57.1)	454.2**
	CO ₂	2	1.4(2.9)	30**	3.2 (14.5)	130**	104 (1.6)	6.4**	2.30 (40.0)	318.0**
	N × CO ₂	4	2.3(4.6)	23**	0.8 (3.5)	15**	219 (3.4)	6.7**	0.22 (0.4)	1.5 ns
	Error	40	1.0(1.9)		0.5 (2.2)		323 (5.0)		0.15 (2.5)	
Maize	N	2	43.9 (96.5)	838**	22.2 (95.2)	529**	123 (90.5)	225.9**	0.97(6.1)	1.4 ns
	CO ₂	2	0.4 (0.9)	7**	0.2 (0.9)	5**	0 (1.3)	3.3*	0.46 (2.9)	0.6 ns
	N × CO ₂	4	0.1 (0.3)	1 ns	0.1 (0.3)	1 ns	0 (0.1)	0.1 ns	0.64 (4.1)	0.4 ns
	Error	40	1.0(2.3)		0.8 (3.6)		1 (8.0)		13.64 (86.8)	

N refers to the three nitrogen-forms effect; *CO*₂ refers to the three *CO*₂ levels effect; *N* × *CO*₂ refers to nitrogen-form × *CO*₂ levels interaction effects. Values in brackets following the sum of squares for variables indicate the percentage (%) of given variation to total variation. * and ** indicate significant at 0.05 and 0.01 level, respectively. *df* refers to the degree of freedom. ns means no significant difference.



CONCLUSION

In conclusion, under ambient CO₂ conditions and AN nutrition, electron transport was reduced in both the C₃ wheat and C₄ maize plants, leading to a suppression of photosynthetic carbon assimilation. In wheat growing under elevated atmospheric CO₂ concentrations (*C_a*), increased *C_i* and *C_c* values improved electron flux to CO₂ assimilation rather than to photorespiration, thus sustaining photosynthesis

and alleviating NH₄⁺-induced stress. In contrast, elevated *C_a* had a negligible effect on *C_i* and *C_s* in maize and, consequently, minor effects on photosynthesis. Therefore, future increases in atmospheric *C_a* should provide C₃ plants with more opportunities to use NH₄⁺ rather than relying on NO₃⁻ as a source of N fertilizers for crop production. Analyses using molecular biology and mutants to explain the possible physiological mechanisms in NH₄⁺ tolerance of crop cultivars.

DATA AVAILABILITY STATEMENT

All datasets generated for this study are included in the manuscript/**Supplementary Material**.

AUTHOR CONTRIBUTIONS

FW and XH conceived the original screening and research plans. FW, JG, and XH supervised the experiments. FW performed most of the experiments, conceived the project, and wrote the article with salient contributions from all the authors in specific areas. FW, JG, JY, QW, JM, and XH supervised and completed the writing. All authors contributed to the article and approved the submitted version.

FUNDING

This work was supported by the 100 Talents Program of Chongqing (20710940) and the World-Class Biological Science

Discipline Development Program at the Southwest University, China (100030/2120054019), the Chinese Postdoctoral Science Foundation (2017M622948) and the Chongqing Postdoctoral Science Foundation (Xm2017147), and Key R & D project of Zhejiang Province “R & D and application of green, safe and efficient fertilizers” (2020R20A50B01).

ACKNOWLEDGMENTS

The authors would like to thank Professor Hans Lambers (School of Biological Sciences, University of Western Australia) for guidance in writing the manuscript.

SUPPLEMENTARY MATERIAL

The Supplementary Material for this article can be found online at: <https://www.frontiersin.org/articles/10.3389/fpls.2020.537443/full#supplementary-material>

REFERENCES

- Anderson, L. J., Maherali, H., Johnson, H. B., Polley, H. W., and Jackson, R. B. (2001). Gas exchange and photosynthetic acclimation over subambient to elevated CO₂ in a C₃-C₄ grassland. *Global Change Biol.* 7, 693–707. doi: 10.1046/j.1354-1013.2001.00438.x
- Andrews, T. J., and Lorimer, G. H. (1978). Photorespiration—still still unavoidable? *FEBS Lett.* 90, 1–9. doi: 10.1016/0014-5793(78)80286-5
- Aranjuelo, I., Pardo, A., Biel, C., Save, R., Azcon-Bieto, J., and Nogues, S. (2009). Leaf carbon management in slow-growing plants exposed to elevated CO₂. *Global Change Biol.* 15, 97–109. doi: 10.1111/j.1365-2486.2008.01829.x
- Ariz, I., Artola, E., Asensio, A. C., Cruchaga, S., Aparicio-Tejo, P. M., and Moran, J. F. (2011). High irradiance increases NH₄⁺ tolerance in *Pisum sativum*: higher carbon and energy availability improve ion balance but not N assimilation. *J. Plant Physiol.* 168, 1009–1015. doi: 10.1016/j.jplph.2010.11.022
- Ariz, I., Asensio, A. C., Zamarreno, A. M., Garcia-Mina, J. M., Aparicio-Tejo, P. M., and Moran, J. F. (2013). Changes in the C/N balance caused by increasing external ammonium concentrations are driven by carbon and energy availabilities during ammonium nutrition in pea plants: the key roles of asparagine synthetase and anaplerotic enzymes. *Physiol. Plant.* 148, 522–537. doi: 10.1111/j.1399-3054.2012.01712.x
- Ariz, I., Esteban, R., García-Plazaola, J. I., Becerril, J. M., Aparicio-Tejo, P. M., and Moran, J. F. (2010). High irradiance induces photoprotective mechanisms and a positive effect on NH₄⁺ stress in *Pisum sativum* L. *J. Plant Physiol.* 167, 1038–1045. doi: 10.1016/j.jplph.2010.02.014
- Balkos, K. D., Britto, D. T., and Kronzucker, H. J. (2010). Optimization of ammonium acquisition and metabolism by potassium in rice (*Oryza sativa* L. cv. IR-72). *Plant Cell Environ.* 33, 23–34.
- Bloom, A. J. (2015). Photorespiration and nitrate assimilation: a major intersection between plant carbon and nitrogen. *Photosynth. Res.* 123, 117–128. doi: 10.1007/s11120-014-0056-y
- Bloom, A. J., Burger, M., Asensio, J. S. R., and Cousins, A. B. (2010). Carbon dioxide enrichment inhibits nitrate assimilation in wheat and *Arabidopsis*. *Science* 328, 899–903. doi: 10.1126/science.1186440
- Bloom, A. J., Burger, M., Kimball, B. A., and Pinter, P. J. (2014). Nitrate assimilation is inhibited by elevated CO₂ in field-grown wheat. *Nat. Clim. Chang.* 4:477. doi: 10.1038/nclimate2183
- Bloom, A. J., Smart, D. R., Nguyen, D. T., and Searles, P. S. (2002). Nitrogen assimilation and growth of wheat under elevated carbon dioxide. *Proc. Natl. Acad. Sci. U. S. A.* 99, 1730–1735. doi: 10.1073/pnas.022627299
- Britto, D. T., and Kronzucker, H. J. (2002). NH₄⁺ toxicity in higher plants: a critical review. *J. Plant Physiol.* 159, 567–584. doi: 10.1078/0176-1617-0774
- Carmo-Silva, E., Scales, J. C., Madgwick, P. J., and Parry, M. A. (2015). Optimizing Rubisco and its regulation for greater resource use efficiency. *Plant, Cell Environ.* 38, 1817–1832. doi: 10.1111/pce.12425
- Conn, S. J., Hocking, B., Dayod, M., Xu, B., Athman, A., Henderson, S., et al. (2013). Protocol: optimising hydroponic growth systems for nutritional and physiological analysis of *Arabidopsis thaliana* and other plants. *Plant Methods* 9:4. doi: 10.1186/1746-4811-9-4
- Coskun, D., Britto, D. T., Shi, W., and Kronzucker, H. J. (2017). Nitrogen transformations in modern agriculture and the role of biological nitrification inhibition. *Nat. Plants* 3:17074.
- Cousins, A. B., and Bloom, A. J. (2003). Influence of elevated CO₂ and nitrogen nutrition on photosynthesis and nitrate photoreduction in maize (*Zea mays* L.). *Plant Cell Environ.* 26, 1525–1530. doi: 10.1046/j.1365-3040.2003.01075.x
- Demmig-Adams, B., and Adams, W. I. I. (1992). Photoprotection and other responses of plants to high light stress. *Ann. Rev. Plant Biol.* 43, 599–626. doi: 10.1146/annurev.pp.43.060192.003123
- Demmig-Adams, B., Winter, K., Krüger, A., and Czygan, F. C. (1989). Light response of CO₂ assimilation, dissipation of excess excitation energy, and zeaxanthin content of sun and shade leaves. *Plant Physiol.* 90, 881–886. doi: 10.1104/pp.90.3.881
- Dier, M., Meinen, R., Erbs, M., Kollhorst, L., Baillie, C. K., Kaufholdt, D., et al. (2018). Effects of free air carbon dioxide enrichment (FACE) on nitrogen assimilation and growth of winter wheat under nitrate and ammonium fertilization. *Global Change Biol.* 24, e40–e54.
- Drath, M., Kloft, N., Batschauer, A., Marin, K., Novak, J., and Forchhammer, K. (2008). Ammonia triggers photodamage of photosystem II in the cyanobacterium *Synechocystis* sp. strain PCC 6803. *Plant Physiol.* 147, 206–215. doi: 10.1104/pp.108.117218
- Edwards, E. J., Osborne, C. P., Strömberg, C. A., Smith, S. A., and Consortium, C. G. (2010). The origins of C₄ grasslands: integrating evolutionary and ecosystem science. *Science* 328, 587–591. doi: 10.1126/science.1177216
- Ehleringer, J. R., Sage, R. F., Flanagan, L. B., and Pearcy, R. W. (1991). Climate change and the evolution of C₄ photosynthesis. *Trends Ecol. Evol.* 6:95. doi: 10.1016/0169-5347(91)90183-x
- Farquhar, G. D., von Caemmerer, ., and Berry, J. (1980). A biochemical model of photosynthetic CO₂ assimilation in leaves of C₃ species. *Planta* 149, 78–90. doi: 10.1007/bf00386231

- Fernández-Crespo, E., Camañes, G., and García-Agustín, P. (2012). Ammonium enhances resistance to salinity stress in citrus plants. *J. Plant Physiol.* 169, 1183–1191. doi: 10.1016/j.jplph.2012.04.011
- Franks, P. J., Adams, M. A., Amthor, J. S., Barbour, M. M., Berry, J. A., Ellsworth, D. S., et al. (2013). Sensitivity of plants to changing atmospheric CO₂ concentration: from the geological past to the next century. *New Phytol.* 197, 1077–1094. doi: 10.1111/nph.12104
- Fryer, M. J., Andrews, J. R., Oxborough, K., Blowers, D. A., and Baker, N. R. (1998). Relationship between CO₂ assimilation, photosynthetic electron transport, and active O₂ metabolism in leaves of maize in the field during periods of low temperature. *Plant Physiol.* 116, 571–580. doi: 10.1104/pp.116.2.571
- Gao, J., Wang, F., Sun, J., Tian, Z., Hu, H., Jiang, S., et al. (2018). Enhanced Rubisco activation associated with maintenance of electron transport alleviates inhibition of photosynthesis under low nitrogen conditions in winter wheat seedlings. *J. Exp. Botany* 69, 5477–5488.
- Genty, B., Briantais, J. M., and Baker, N. R. (1989). The relationship between the quantum yield of photosynthetic electron transport and quenching of chlorophyll fluorescence. *Biochim. Biophys. Acta Gen. Subj.* 990, 87–92. doi: 10.1016/s0304-4165(89)80016-9
- Ghannoum, O., Caemmerer, S., Ziska, L. H., and Conroy, J. P. (2000). The growth response of C₄ plants to rising atmospheric CO₂ partial pressure: a reassessment. *Plant Cell Environ.* 23, 931–942. doi: 10.1046/j.1365-3040.2000.00609.x
- Ghannoum, O., von Caemmerer, S., Barlow, E. W., and Conroy, J. P. (1997). The effect of CO₂ enrichment and irradiance on the growth, morphology and gas exchange of a C₃ (*Panicum laxum*) and a C₄ (*Panicum antidotale*) grass. *Funct. Plant Biol.* 24, 407–407. doi: 10.1071/pp96077_co
- Gong, P., Liang, L., and Zhang, Q. (2011). China must reduce fertilizer use too. *Nature* 473, 284–285. doi: 10.1038/473284e
- Hatch, M. D., and Slack, C. R. (1966). Photosynthesis by sugar-cane leaves: a new carboxylation reaction and the pathway of sugar formation. *Biochem. J.* 101, 103–111. doi: 10.1042/bj1010103
- IPCC (2007). *Agriculture: Contribution of Working Group III to the Fourth Assessment Report of the Intergovernmental Panel on Climate Change*, eds B. Metz, O. R. Davidson, P. R. Bosch, R. Dave, and L. A. Meyer (Cambridge, New York, NY: Cambridge University Press), 497–540.
- IPCC (2013). *Climate Change 2013: The Physical Science Basis. Contribution of Working Group I to the Fifth Assessment Report of the Intergovernmental Panel on Climate Change*, eds T. F. Stocker, D. Qin, G. K. Plattner, M. Tignor, S. K. Allen, J. Boschung, et al. (Cambridge, New York, NY: Cambridge University Press).
- Johnson, M. P., Goral, T. K., Duffy, C. D., Brain, A. P., Mullineaux, C. W., and Ruban, A. V. (2011). Photoprotective energy dissipation involves the reorganization of photosystem II light-harvesting complexes in the grana membranes of spinach chloroplasts. *Plant Cell* 23, 1468–1479. doi: 10.1105/tpc.110.081646
- Jordan, D. B., and Ogren, W. L. (1984). The CO₂/O₂ specificity of ribulose 1, 5-bisphosphate carboxylase/oxygenase. *Planta* 161, 308–313.
- Kanemoto, K., Yamashita, Y., Ozawa, T., Imanishi, N., Nguyen, N. T., Suwa, R., et al. (2009). Photosynthetic acclimation to elevated CO₂ is dependent on N partitioning and transpiration in soybean. *Plant Sci.* 177, 398–403. doi: 10.1016/j.plantsci.2009.06.017
- Kim, C., and Apel, K. (2013). Singlet oxygen-mediated signaling in plants: moving from flu to wild type reveals an increasing complexity. *Photosynth. Res.* 116, 455–464. doi: 10.1007/s11120-013-9876-4
- Kramer, D. M., Johnson, G., Kiirats, O., and Edwards, G. E. (2004). New fluorescence parameters for the determination of QA redox state and excitation energy fluxes. *Photosynth. Res.* 79:209. doi: 10.1023/b:pres.0000015391.99477.0d
- Kühlbrandt, W., Wang, D. N., and Fujiyoshi, Y. (1994). Atomic model of plant light-harvesting complex by electron crystallography. *Nature* 367, 614–621. doi: 10.1038/367614a0
- Leakey, A. D., Uribealrrea, M., Ainsworth, E. A., Naidu, S. L., Rogers, A., Ort, D. R., et al. (2006). Photosynthesis, productivity, and yield of maize are not affected by open-air elevation of CO₂ concentration in the absence of drought. *Plant Physiol.* 140, 779–790. doi: 10.1104/pp.105.073957
- Li, B., Shi, W., and Su, Y. (2011). The differing responses of two *Arabidopsis* ecotypes to ammonium are modulated by the photoperiod regime. *Acta Physiol. Plant.* 33, 325–334. doi: 10.1007/s11738-010-0551-5
- Li, H., Wang, Y., Xiao, J., and Xu, K. (2015). Reduced photosynthetic dark reaction triggered by ABA application increases intercellular CO₂ concentration, generates H₂O₂ and promotes closure of stomata in ginger leaves. *Environ. Exp. Bot.* 113, 11–17. doi: 10.1016/j.envexpbot.2015.01.002
- Li, Y., Gao, Y., Xu, X., Shen, Q., and Guo, S. (2009). Light-saturated photosynthetic rate in high-nitrogen rice (*Oryza sativa* L.) leaves is related to chloroplastic CO₂ concentration. *J. Exp. Bot.* 60, 2351–2360. doi: 10.1093/jxb/erp127
- Lloyd, J., and Farquhar, G. D. (1996). The CO₂ dependence of photosynthesis, plant growth responses to elevated atmospheric CO₂ concentrations and their interaction with soil nutrient status. I. General principles and forest ecosystems. *Funct. Ecol.* 10, 4–32. doi: 10.2307/2390258
- Long, S. P., and Bernacchi, C. J. (2003). Gas exchange measurements, what can they tell us about the underlying limitations to photosynthesis? Procedures and sources of error. *J. Exp. Bot.* 54, 2393–2401. doi: 10.1093/jxb/erg262
- Medlyn, B., Barton, C. V. M., Broadmeadow, M. S. J., Ceulemans, R., De Angelis, P., Forstreuter, M., et al. (2001). Stomatal conductance of forest species after long-term exposure to elevated CO₂ concentration: a synthesis. *New Phytol.* 149, 247–264. doi: 10.1046/j.1469-8137.2001.00028.x
- Mehrer, I., and Mohr, H. (1989). Ammonium toxicity: description of the syndrome in *Sinapis alba* and the search for its causation. *Physiol. Plant.* 77, 545–554. doi: 10.1111/j.1399-3054.1989.tb05390.x
- Miller, A. J., and Cramer, M. D. (2005). Root nitrogen acquisition and assimilation. *Plant Soil* 274, 1–36. doi: 10.1007/1-4020-4099-7_1
- Nguyen, N. T., McInturf, S. A., and Mendoza-Cózatl, D. G. (2016). Hydroponics: a versatile system to study nutrient allocation and plant responses to nutrient availability and exposure to toxic elements. *J. Vis. Exp.* 113:e54317.
- Onoda, Y., Hikosaka, K., and Hirose, T. (2004). Allocation of nitrogen to cell walls decreases photosynthetic nitrogen-use efficiency. *Funct. Ecol.* 18, 419–425. doi: 10.1111/j.0269-8463.2004.00847.x
- Owensby, C. E., Ham, J. M., Knapp, A. K., and Auen, L. M. (1999). Biomass production and species composition change in a tallgrass prairie ecosystem after long-term exposure to elevated atmospheric CO₂. *Global Change Biol.* 5, 497–506. doi: 10.1046/j.1365-2486.1999.00245.x
- Richter, J., and Roelcke, M. (2000). The N-cycle as determined by intensive agriculture—examples from central Europe and China. *Nutr. Cycl. Agroecosyst.* 57, 33–46.
- Robredo, A., Pérez-López, U., Miranda-Apodaca, J., Lacuesta, M., Mena-Petite, A., and Muñoz-Rueda, A. (2011). Elevated CO₂ reduces the drought effect on nitrogen metabolism in barley plants during drought and subsequent recovery. *Environ. Exp. Bot.* 71, 399–408. doi: 10.1016/j.envexpbot.2011.02.011
- Sage, R. F. (2004). The evolution of C₄ photosynthesis. *New Phytol.* 161, 341–370.
- Setien, I., Fuertes-Mendizabal, T., Gonzalez, A., Aparicio-Tejo, P. M., Gonzalez-Murua, C., Gonzalez-Moro, M. B., et al. (2013). High irradiance improves ammonium tolerance in wheat plants by increasing N assimilation. *J. Plant Physiol.* 170, 758–771. doi: 10.1016/j.jplph.2012.12.015
- Shikanai, T. (2011). Regulation of photosynthetic electron transport. *Biochim. Biophys. Acta* 1807, 375–383.
- von Caemmerer, S., and Farquhar, G. D. (1999). “The modelling of C₄ photosynthesis,” in *The Biology of C₄ Photosynthesis*, ed. R. M. Sage (New York, NY: Academic Press), 173–211.
- Wang, F., Gao, J., Liu, Y., Tian, Z., Muhammad, A., Zhang, Y., et al. (2016a). Higher ammonium transamination capacity can alleviate glutamate inhibition on winter wheat (*Triticum aestivum* L.) root growth under high ammonium stress. *PLoS One* 11:e0160997. doi: 10.1371/journal.pone.0160997
- Wang, F., Gao, J., Shi, S., He, X., and Dai, T. (2019). Impaired electron transfer accounts for the photosynthesis inhibition in wheat seedlings (*Triticum aestivum* L.) subjected to ammonium stress. *Physiol. Plant.* 167, 159–172. doi: 10.1111/ppl.12878
- Wang, F., Gao, J., Tian, Z., Liu, Y., Abid, M., Jiang, D., et al. (2016b). Adaptation to rhizosphere acidification is a necessary prerequisite for wheat (*Triticum aestivum* L.) seedling resistance to ammonium stress. *Plant Physiol. Biochem.* 108, 447–455. doi: 10.1016/j.plaphy.2016.08.011

- Xing, G., and Zhu, Z. (2000). An assessment of N loss from agricultural fields to the environment in China. *Nutr. Cycl. Agroecosyst.* 57, 67–73.
- Xu, G., Fan, X., and Miller, A. J. (2012). Plant nitrogen assimilation and use efficiency. *Ann. Rev. Plant Biol.* 63, 153–182. doi: 10.1146/annurev-arplant-042811-105532
- Yong, J. W. H., Letham, D. S., Wong, S. C., and Farquhar, G. D. (2010). Effects of root restriction on growth and associated cytokinin levels in cotton (*Gossypium hirsutum*). *Funct. Plant Biol.* 3, 974–984. doi: 10.1071/fp10009
- Yong, J. W. H., Wong, S. C., and Farquhar, G. D. (1997). Stomatal responses to changes in vapour pressure difference between leaf and air. *Plant Cell Environ.* 20, 1213–1216. doi: 10.1046/j.1365-3040.1997.d01-27.x
- Yong, J. W. H., Wong, S. C., Letham, D. S., Hocart, C. H., and Farquhar, G. D. (2000). Effects of elevated CO₂ and nitrogen nutrition on cytokinins in the xylem sap and leaves of cotton. *Plant Physiol.* 124, 767–780. doi: 10.1104/pp.124.2.767
- Zhou, Y. H., Yu, J. Q., Huang, L. F., and Nogues, S. (2004). The relationship between CO₂ assimilation, photosynthetic electron transport and water-water cycle in chill-exposed cucumber leaves under low light and subsequent recovery. *Plant Cell Environ.* 27, 1503–1514. doi: 10.1111/j.1365-3040.2004.01255.x

Conflict of Interest: The authors declare that the research was conducted in the absence of any commercial or financial relationships that could be construed as a potential conflict of interest.

Copyright © 2020 Wang, Gao, Yong, Wang, Ma and He. This is an open-access article distributed under the terms of the Creative Commons Attribution License (CC BY). The use, distribution or reproduction in other forums is permitted, provided the original author(s) and the copyright owner(s) are credited and that the original publication in this journal is cited, in accordance with accepted academic practice. No use, distribution or reproduction is permitted which does not comply with these terms.